Journal of Magnetics 19(4), 340-344 (2014)

ISSN (Print) 1226-1750
ISSN (Online) 2233-6656
http://dx.doi.org/10.4283/JMAG.2014.19.4.340

Study on the Magnetic Characteristics of Anisotropic $SmCo_7$-type Alloys Synthesized by High-energy Surfactant-assisted Ball Milling

N. J. Yu[1], P. Y. Zhang[1]*, Y. J. Shi[1]*, M. X. Pan[1], S. Y. Zhang[1], H. L. Ge[1], and Y. C. Lu[2]

[1]*Magnetism Key Laboratory of Zhejiang Province, China Jiliang University, Hangzhou 310018, China*
[2]*Zhejiang Kevin Magnet Co. Ltd, Dongyang 322105, China*

(Received 4 July 2014, Received in final form 16 August 2014, Accepted 11 September 2014)

An effective process was employed for synthesizing anisotropic magnetic $SmCo_7$-type alloy flakes with high coercivity, which is highly desirable for many applications. The highest coercivity of 16.3 kOe corresponds to a typical flake thickness of 200 nm for the 3-h ball-milled sample. The anisotropy field was calculated by measuring the parallel and perpendicular directions to the easy magnetization direction of the powders. The anisotropy field decreased with the increase of the ball milling time, thus indicating that the decrease of coercivity was mainly caused by the reduction of the anisotropy field. Microstructure analysis indicated that the morphology, grain size, and anisotropy field of these samples have a great influence on the magnetic properties.

Keywords : $SmCo_7$-type alloy, magnetic properties, grain size, anisotropy field

1. Introduction

Rare earth cobalt-based intermetallic compounds have potential applications as permanent magnets owing to their distinctive electronic structure. Since the 1970s, Sm-Co-based permanent magnets have drawn considerable interest due to their highly attractive properties including high energy density, reliable coercive force, high anisotropy, best high-temperature performance, relatively good corrosion, and oxidation resistance. These excellent performances have made Sm-Co alloys suitable materials for high temperature applications [1, 2]. Of these Sm-Co intermetallics, $SmCo_5$- and Sm_2Co_{17}-type alloys have been studied more extensively as high temperature candidate materials for permanent magnets [3-7].

However, the Sm_2Co_{17}-type alloys have shortcomings of a low intrinsic coercivity and low operating temperature [8] whereas the disadvantages of the $SmCo_5$-type alloys are their relatively lower Curie temperature and magnetic moment [9]. In comparison, the $Sm(Co,M)_7$ (M = stabilizing element) compounds with the $TbCu_7$-type structure (space group P6/mmm) possess a higher predicted Curie temperature, a high magnetic anisotropy field, and a low intrinsic coercivity temperature coefficient [10]. Thus, the $SmCo_7$-type alloys could be suitable for development as permanent magnets for high temperature applications.

In the last few years, there has been great scientific interest in $SmCo_7$-type alloys due to their potential applications as novel high temperature, rare earth permanent magnets [11-14]. However, pure $SmCo_7$ phase is metastable, and it cannot be obtained by general equilibrium methods. Thus, a third element is usually doped to stabilize the $SmCo_7$-type phase and improve its magnetic properties. A small amount of the third element (i.e. Cu, Zr, Ti, Hf, and Si) can stabilize the Sm-Co phase with the $TbCu_7$-type structure [6-10]. Hence, Cu and Zr were doped as the third elements to stabilize the $SmCo_7$-type phase in this paper.

It is reported that $SmCo_7$-type alloys have lower coercivity by a general mechanically alloyed method [14]. Recently, the best performance of magnetic properties occurs in textured materials where the easy magnetization axes are all aligned, which increase their remanence and magnetic energy product [16]. This result may inspire a good method to fabricate textured structure in $SmCo_7$-type alloys in order to obtain better performance of magnetic properties such as coercivity. Additionally, the concept of textured exchange-spring type magnets was proposed in the early 1990s [17-19].

*Corresponding author: Tel: +86-0571-8767-6292
Fax: +86-0571-2888-9526, e-mail: pyzhang_cjlu@163.com

The basic principle in the nano-composite hard magnets is to exchange a coupled, nanoscale textured, hard magnetic phase having high coercivity with a nanosized soft phase of very large magnetization [20, 21]. Techniques including unidirectional solidification, deformation-induced texture, magnetic field-assisted ball-milling, and melt-spinning at low wheel speeds have induced texture in Sm-Co alloys either with low degree of texture or with a moderate degree of texture resulting in a non-unidirectional easy axis [22-25].

This paper presents the preparation and characterization of $SmCo_7$-type alloys with out-of-plane texture. A technique of high energy ball milling with surfactant assistance was employed to prepare magnetically anisotropy $SmCo_7$-type alloy powders. The microstructure, magnetical anisotropy, and magnetic properties of the $Sm(Co,Fe,Cu,Zr)_{7.88}$ flakes were investigated.

2. Experimental Details

The alloys with the nominal composition of $Sm(Co_{0.84}$-$Fe_{0.05}Cu_{0.09}Zr_{0.02})_{7.88}$ were prepared by arc melting in a high purity argon atmosphere. An excess Sm of 25 wt.% was added to each sample to compensate for the loss of Sm during the process. The ingots were turned upside down and melted three times to ensure homogeneity. The as-cast ingots were crushed into coarse powder with typical sizes less than 200 μm. The powder was milled by a high-energy SPEX 8000 mixer/mill with a ratio of powder to ball of 1:8-12 in weight for 1 h, 3 h, 5 h, and 8 h, respectively. Powders were handled in an argon box to prevent oxidation. Heptanes solvent was used as the solvent with a 65% powder weight. Oleic acid was used as the surfactant with a 20% powder weight. After milling, the powders were washed with heptanes solvent. Powders and as-cast ingots were dried in vacuum, mixed with epoxy in polyurethane mold, and then magnetically aligned using a pulse field of 5 T before being left to cure in a field of 1.5 T to assure the alignment.

A vibrating-sample magnetometer (VSM) and a superconducting quantum interference device (SQUID) were used for magnetic measurements along both directions parallel and perpendicular to the magnetic-aligned direction. An X-ray diffraction equipment (XRD) was used for characterizing the crystal structure. Scanning Electron Microscope (SEM) and Transmission Electron Microscopy (TEM) images were studied to determine the powder morphology and evaluate the particle sizes.

3. Results and Discussion

Figure 1(a) and (b) illustrate the demagnetization curves of the pre-aligned $Sm(Co,Fe,Cu,Zr)_{7.88}$ powder samples and the as-cast starting alloy tested using a VSM along both parallel (//) and perpendicular (⊥) to the magnetic aligning direction. These results demonstrated how the ball milling time affected the remanence B_r and coercivity H_{cj}. All samples are magnetically hard; however, in some cases, the existence of the step at the field reversal point distorted the loop squareness in Fig. 1(a), thereby indicating a separate-switching behavior of the hard- and soft-magnetic phases. For 5-h ball-milled, aligned powder samples, the demagnetization curve showed a nearly single hard-magnetic phase behavior, thus indicating a good exchange-coupling between the hard- and soft- magnetic phase in this sample. However, the remanence B_r value and the coercivity H_{cj} value for the 5-h ball-milled sample is much lower than that of 1-h and 3-h milled samples. As shown in Fig. 1(a), for the parallel direction, the remanence B_r values decreased when ball milling time increased from 1 h to 8 h. The maximum remanence B_r was about 8.49 kG for the 1 h ball-milled powder sample.

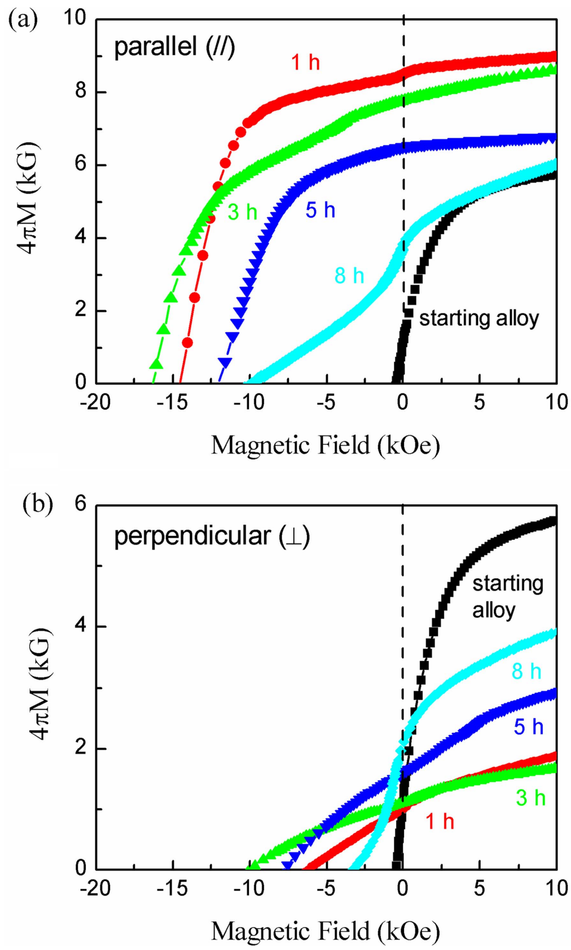

Fig. 1. (Color online) Demagnetization curves of the aligned $Sm(Co,Fe,Cu,Zr)_{7.88}$ powder samples and the starting alloy: (a) parallel to EMD; (b) perpendicular to EMD.

However, no obvious variation between coercivity H_{cj} values and ball milling time occurred. The maximum coercivity H_{cj} value was about 16.3 kOe for the 3-h ball-milled powder sample, and further milling resulted in a decrease in coercivity. For the perpendicular direction, as shown in Fig. 1(b), the remanence B_r values showed an opposite behavior. The remanence B_r values increased gradually as the ball milling time increased from 1 h to 8 h. It has the lowest value 1.01 kG of B_r for 1-h ball-milled powder sample. The values of H_{cj} also show no obvious variation with ball milling time. The maximum coercivity H_{cj} value was also for the 3-h ball-milled powder sample, which is about 10.0 kOe. The variations of coercivity H_{cj} and remanence B_r with ball milling times are illustrated in Fig. 2, respectively. Fig. 2(a) shows the magnetic properties of the original ball-milled powder samples. Both parallel (//) and perpendicular (⊥) directions to the easy magnetization direction (EMD) are presented in Figs. 2(b) and (c). As shown in Fig. 2, it is indicated that the coercivity H_{cj} and remanence B_r were significantly affected by ball milling time. The variations of the coercivity H_{cj} were similar between parallel (//) and perpendicular (⊥) directions to EMD. The same behavior of coercivity H_{cj} was found in the original ball-milled samples. Nevertheless the variations of remanence B_r were opposite between the two orientations.

Figure 3 displays the XRD patterns of the pre-aligned $Sm(Co,Fe,Cu,Zr)_{7.88}$ powder samples and the as-cast alloy along the perpendicular and parallel directions to the EMD, respectively. As shown in Fig. 3(a), it can be seen that the main phase was the Sm-Co 1:7 with $TbCu_7$-type structure, and the pre-aligned as-cast alloy was randomly oriented. The result of the XRD indicated that addition of a small amount of Cu and Zr contributed to obtaining the $SmCo_7$-type phase. The XRD patterns presented in Fig. 3(a) also show a strong *c*-axis (002) out-of-plane crystal texture in all ball-milled samples. It can be noted that, with the increase of ball milling time from 1 h to 8 h, the intensity of the out-of-plane (002) texture component decreased monotonically. The presence of a strong (002) peak indicated that the flakes exhibited a uniaxial magnetocrystalline anisotropy. Fig. 3(b) shows the XRD patterns of these samples parallel (//) to the EMD. As shown in the Fig. 3(b), a strong (200) peak was presented. With the increase of ball milling time, the peak intensity of XRD decreased, and the peak broadening increased both in Fig. 3(a) and (b), thus indicating a decrease in grain size and an increase in the degree of amorphization.

The $SmCo_{7-x}M_x$ intermetallics exhibited strong uniaxial magnetocrystalline anisotropy with an anisotropy field more than 200 kOe at 5 K [1]. The anisotropy field can be experimentally determined from the intersection point of two extrapolated magnetization curves with the applied field parallel and perpendicular to the EMD of powder, which was fixed with epoxy and then pre-aligned in a magnetic field when it was solidifying [1]. Fig. 4(a) shows typical anisotropy fields of $Sm(Co_{0.84}Fe_{0.05}Cu_{0.09}Zr_{0.02})_{7.88}$ intermetallic compounds, and the inset shows the XRD patterns of the pre-aligned powder samples, which presents a strong (002) peak. This strong peak indicated that the $SmCo_7$-type powder exhibited a strong

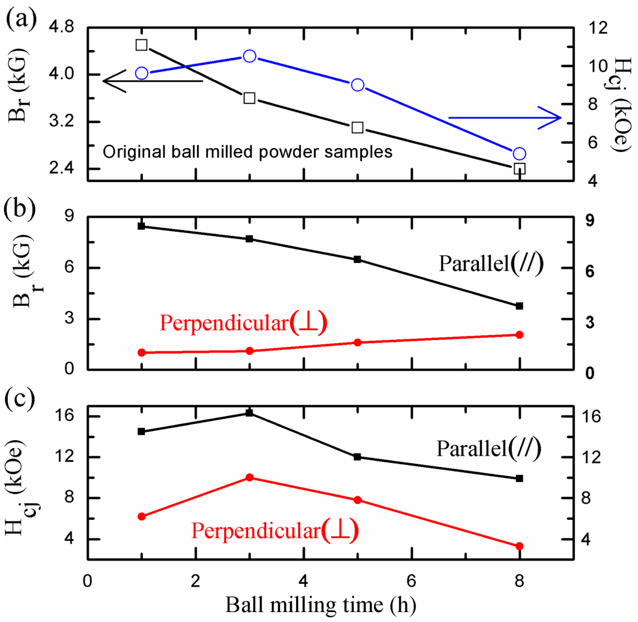

Fig. 2. (Color online) The variation of magnetic properties with ball milling time of: (a) the original balled samples, (b) coercivity H_{cj}, (c) remanence B_r.

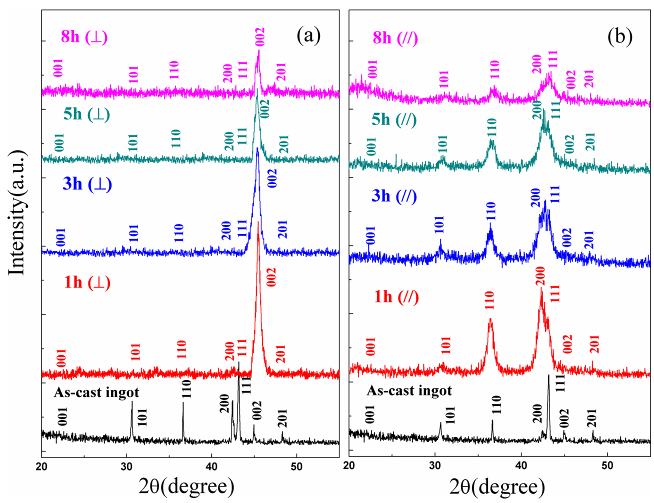

Fig. 3. (Color online) The XRD patterns of the aligned $Sm(Co,Fe,Cu,Zr)_{7.88}$ powder samples and the as-cast ingot: (a) perpendicular to EMD; (b) parallel to EMD.

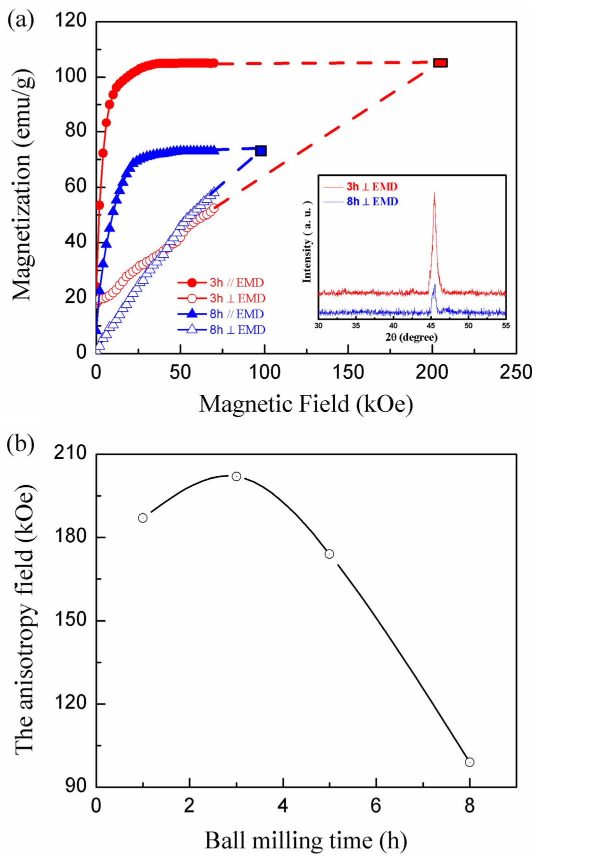

Fig. 4. (Color online) (a) The anisotropy field measurement at 5K for the aligned powder samples of $Sm(Co,Fe,Cu,Zr)_{7.88}$, the inset shows the XRD pattern for the aligned samples. (b) The variation of the anisotropy field of the aligned ball milled powder samples.

uniaxial magnetocrystalline anisotropy. As shown in Fig. 4, the $Sm(Co_{0.84}Fe_{0.05}Cu_{0.09}Zr_{0.02})_{7.88}$ powder illustrates a high anisotropy field of about 202 kOe for the 3-h ball-milling powder sample at 5 K. However, the anisotropy field (H_A) of the 8-h ball-milling powder sample decreased to 99 kOe at 5 K. Fig. 4(b) indicates that when the ball milling time exceeded 3 h, the anisotropy field decreased rapidly with the increase of ball milling time.

In order to discover the relationship among the grain size, particle size, and the anisotropy field, TEM and SEM images of samples were studied to evaluate the grain size and particle size of the 3-h and 8-h ball-milled powder samples, respectively. Fig. 5 shows the morphology of the ball-milled powder samples. Fig. 5(a) and (b) are the SEM micrographs of ball-milled samples for 3 h and 8 h, respectively, while Fig. 5(c) and (d) are the TEM micrographs of ball milled samples for 3 h and 8 h, respectively. Fig. 5(c) and (d) show that the average grain size of milled samples decreased rapidly from 90 nm for 3 h to 7 nm for 8 h, thus indicating that the grain size decreased rapidly when the ball milling time increased. Additionally, G. B. Han *et al.* pointed out that the effective anisotropy decreases with the reduction of the grain size and decreases dramatically when the grain size is smaller than the thickness of the domain wall L_{ex} [26]. This decrease of the coercivity was mainly caused by the reduction of the effective anisotropy. According to results in Fig. 4 and Fig. 5, the decreased anisotropy field in our samples was mainly caused by the grain size decreased from 90 nm to 7 nm. In addition, as shown in Fig. 5(a)

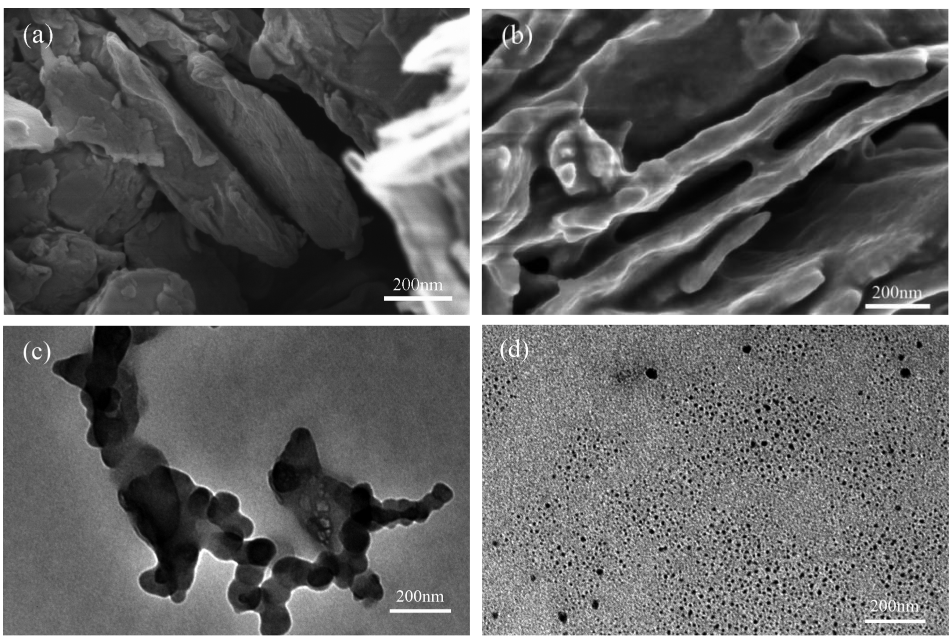

Fig. 5. SEM micrographs of ball milled samples: (a) 3 h, (b) 8 h; TEM micrographs of ball milling samples: (c) 3 h, (d) 8 h.

and (b), the thickness of the ball-milled flakes decreased from 300 nm to 80 nm, thus indicating the thickness of these anisotropic flakes obtained by high energy ball milled significantly impacted the magnetic properties.

4. Conclusions

In summary, an effective process using surfactant-assisted high energy ball milling was adopted to obtain $Sm(Co,Fe,Cu,Zr)_{7.88}$ flakes with high magnetic properties. These $Sm(Co,Fe,Cu,Zr)_{7.88}$ flakes had strong magnetic anisotropy. The highest anisotropy field was about 202 kOe for the 3-h ball-milled powder at 5 K The anisotropy field decreased with an increase in ball milling time, thus indicating that the decrease of coercivity was mainly caused by the reduction of the anisotropy field. High coercivity of 16.3 kOe was obtained for the 3-h ball-milled sample. Further milling caused amorphization and resulted in decreases in coercivity and remanence due to the decrease of the anisotropy field.

Acknowledgements

This work was supported by Project of Zhejiang Province Innovative Research Team (No. 2010R50016), Provincial Major Science and Technology Project (No. 2009C21010), the Provincial Natural Science Foundation (No. Z4090462 and Y6100640), the National Science Foundation of China (No. 51001092), and the National Public Interest Research Special (No. 201210107).

References

[1] Y. Q. Guo, W. Li, J. Luo, W. C. Feng, and J. K. Liang, J. Magn. Magn. Mater. **303**, e367 (2006).
[2] T. V. Jayaraman and J. E. Shield, Acta Mater. **60**, 1184 (2012).
[3] K. J. Steant, G. Hoffer, J. Oison, W. Ostertag, and J. J. Becker, J. Appl. Phys. **38**, 1001 (1967).
[4] K. J. Strant and R. M. W. Strant, J. Magn. Magn. Mater. **100**, 38 (1991).
[5] A. E. Ray, J. Appl. Phys. **55**, 2094 (1984).
[6] K. H. J. Buschow and A. S. van der Goot, J. Less-Common Met. **14**, 323 (1968).
[7] R. K. Mishra, G. Thomas, T. Yoneyama, A. Fukino, and T. Ojima, J. Appl. Phys. **52**, 2517 (1981).
[8] G. C. Hadjipanayis, W. Tang, Y. Zhang, et al., IEEE Trans. Magn. **36**, 3382 (2000).
[9] Y. Zhang, Q. Zeng, and G. C. Hadjipanayis, J. Appl. Phys. **97**, 10H107-3 (2005).
[10] Y. Q. Guo, W. C. Feng, and W. Li, J. Appl. Phys. **101**, 023919-7 (2007).
[11] M. Q. Huang, W. E. Wallace, W. E. Mchenry, Q. Chen, and B. M. Ma, J. Appl. Phys. **83**, 6718 (1998).
[12] I. A. Al-Omari, Y. Yeshurun, J. Zhou, and D. J. Sellmyer, J. Appl. Phys. **87**, 6710 (2000).
[13] J. Zhou, I. A. Al-Omari, J. P. Liu, and D. J. Sellmyer, J. Appl. Phys. **87**, 5299 (2000).
[14] J. Luo, J. K. Liang, Y. Q. Guo, Q. L. Liu, L. T. Yang, F. S. Liu, et al. Appl. Phys. Lett. **84**, 3094 (2004).
[15] J. Luo, J. K. Liang, Y. Q. Guo, Q. L. Liu, L. T. Yang, F. S. Liu, Y. Zhang, et al. Appl. Phys. Lett. **85**, 5299 (2004).
[16] K. S. Pal, L. Schultz, and O. Gutfleisch, J. Appl. Phys. **113**, 013913 (2013).
[17] G. C. Hadjipanayis, J. Magn. Magn. Mater. **200**, 373 (1999).
[18] J. M. D. Coey, J. Magn. Magn. Mater. **140-144**, 1041 (1995).
[19] J. P. Liu, F. R. de Boer, P. F. de Châtel, R. Coehoorn, and K. H. J. Buschow, J. Magn. Magn. Mater. **132**, 159 (1994).
[20] E. F. Kneller and R. Hawig, IEEE Trans. Magn. **27**, 3588 (1991).
[21] R. Skomski and J. M. D. Coey, Phys. Rev. B **48**, 15812 (1993).
[22] A. M. Gabay, M. Marinescu, J. F. Liu, and G. C. Hadjipanayis, J. Magn. Magn. Mater. **321**, 3318 (2009).
[23] N. Pligaru, J. Rubin, and J. Bartolome, J. Alloys Compd. **433**, 129 (2007).
[24] C. Rong, V. V. Nguyen, and J. P. Liu, J. Appl. Phys. **107**, 09A717 (2010).
[25] A. Yan, W. Y. Zhang, H. W. Zhang, and B. G. Shen, J. Magn. Magn. Mater. **210**, L10 (2000).
[26] G. B. Han, R. W. Gao, S. S. Yan, H. Q. Liu, S. Fu, W. C. Feng, W. L, and X. M. Li, J. Magn. Magn. Mater. **281**, 6 (2004).